Epoxidation of 1-octene with *tert*-butyl hydroperoxide catalyzed by ZrO_2/Aerosil-SiO_2

Hiroyoshi Kanai [a,*], Yasuhiro Okumura [b], Kazunori Utani [b], Kazuhiko Hamada [c] and Seiichiro Imamura [b,*]

[a] *Department of Environmental Information, Kyoto Prefectural University, Shimogamo, Sakyo-ku, Kyoto 606-8522, Japan*
[b] *Department of Chemistry, Kyoto Institute of Technology, Matsugasaki, Sakyo-ku, Kyoto 606-8585, Japan*
E-mail: imamura@ipc.kit.ac.jp
[c] *Research Division, Pias Corporation, 3-1, 1-Chome, Murotani, Nishi-ku, Kobe 651-2241, Japan*

Received 8 May 2001; accepted 12 July 2001

Oxidation of 1-octene was carried out with *tert*-butyl hydroperoxide at 343 K over ZrO_2/Aerosil-SiO_2. Loading of less than 10 mol% of ZrO_2 on ultrafine Aerosil-SiO_2 gave exclusively 1,2-epoxyoctane. The pre-edge peak area of Zr K-edge XANES and g values of the ESR signals of O_2^- species on ZrO_2/SiO_2 discriminate structures of ZrO_2. On the basis of these analyses it is concluded that the coordinatively unsaturated zirconium oxide is responsible for the selective epoxidation of 1-octene with *tert*-butyl hydroperoxide.

KEY WORDS: epoxidation; ZrO_2/SiO_2; 1-octene; *tert*-butyl hydroperoxide; XANES; ESR; Aerosil-SiO_2

1. Introduction

There is a trend toward the use of heterogeneous catalysts in the selective epoxidation of olefins. One is a group of molecular sieve catalysts containing redox metal ions incorporated in the framework [1]. Another is a group of supported metals or metal oxides which are sophisticatedly prepared to have a specific structure for activating oxidants such as molecular oxygen or peroxides [2–7].

We have been exploiting active and selective olefin epoxidation catalysts with *tert*-butyl hydroperoxide (abbreviated as TBHP) as an oxidant [3–7]. From the previous results we have speculated that early-transition metal oxides with tetrahedral configuration loaded on high surface area supports are active and selective for the reaction. We briefly reported that low-loaded ZrO_2/SiO_2 which was prepared by a sol–gel method is effective for epoxidation of 1-octene [7]. The epoxide selectivity, however, was much inferior to that by TiO_2–SiO_2 [3–5].

There is patent literature on the epoxidation of 1-octene and cyclohexenes with TBHP over ZrO_2/SiO_2 [8], but no information on active species was cited. In the present work, we found that low-loaded ZrO_2 on the ultrafine Aerosil-SiO_2 developed by Degussa-Huls, Corp. is an efficient catalyst for the selective epoxidation of 1-octene with TBHP. On the basis of XAFS and ESR analyses we have clarified that coordinatively unsaturated zirconium oxide is an active species.

2. Experimental

An aqueous solution of 70% *tert*-butyl hydroperoxide (Gift from Nippon Oil & Fats Co.) was mixed with benzene and shaken. The oil layer was dried with anhydrous $MgSO_4$ (Wako Chemicals Co.) and stored over molecular sieve 5A. 1-octene (Nacalai Tesque Co.) was used without further purification.

Aerosil silica (Aerosil 300CF) which was manufactured by thermolysis of $SiCl_4$ in the presence of an O_2–H_2 mixture at Nippon Aerosil Co. was used without further purification. The ZrO_2/SiO_2 catalysts were prepared by impregnating the silica with an aqueous solution of zirconium oxynitrate. The suspension was evaporated with a rotary evaporator, followed by drying overnight at 353 K and heating at 823 K in air for 3 h. The loading of ZrO_2 is in the range of 1–20 mol%. Pure ZrO_2 was prepared by hydrolysis of zirconium oxynitrate with ammonia. A 3 M aqueous solution of ammonia was added to an aqueous solution of zirconium oxynitrate until the pH was 11. The precipitate was filtered and washed with water until the pH of the solution became near neutral followed by drying overnight at 353 K and subsequent heating in air at 823 K for 3 h.

The acid strength of ZrO_2–SiO_2 was measured in dry benzene by using the following Hammett indicators: methyl red ($pK_a = 4.8$), *p*-dimethylaminoazobenzene ($pK_a = 3.3$), benzeneazodiphenylamine ($pK_a = 1.5$), dicinnamalacetone ($pK_a = -3.0$), benzalacetophenone ($pK_a = -5.6$) and anthraquinone ($pK_a = -8.2$). The acid amount was estimated by the titration with 0.01 M *n*-butylamine in benzene.

ZrO_2/SiO_2 powder was placed into a $3 \times 12 \times 20$ mm glass cell, heated *in vacuo* at 473 K for 1 h, and sealed. XAFS spectra were measured at 297 K in a transmission mode at the BL-10B beam line of the Photon Factory in the Institute of Materials Structure Science, High Energy Accelerator Research Organization (KEK-IMSS-PF). The incident beam (300–400 mA) was monochromatized using an Si(311) channel cut crystal.

* To whom correspondence should be addressed.

1 ml of TBHP benzene solution was added to the ZrO_2/SiO_2 powder (150 mg) in an N_2 atmosphere and the mixture was allowed to stand for 3 h, followed by evacuation at room temperature. ESR measurements were carried out at 293 K with a Jeol JES-TE300 ESR spectrometer.

1-octene (10 ml) and 0.2 g of ZrO_2/SiO_2 were added into a three-necked 50 ml flask under an N_2 atmosphere. To this mixture 0.2 ml of benzene solution containing 50% TBHP was added and the flask was maintained at 343 K for periods up to 5 h. The conversion of TBHP was estimated by iodometry. The yield of epoxide was calculated by the analysis using the hydrochloric acid–pyridine method [9].

3. Results and discussion

3.1. Acidity

Silica or ZrO_2 itself has very weak acidity. A small amount of ZrO_2 loading on Aerosil-SiO_2 enhances acid strength and increases acidity especially in the range of $-3.0 < H_0 < +1.5$ (table 1, figure 1). Dang *et al.* reported that Lewis acid sites were generated on ZrO_2/SiO_2 on the basis of the NH_3 and pyridine adsorption analysis [10]. They concluded that newly formed Si–O–Zr bonds are responsible for the Lewis acid sites.

The curve in figure 1 has a maximum at 2–5% of ZrO_2. We can assume that Si–O–Zr linkages should contribute to Lewis acididy which is correlated with both the abundance of Si–O–Zr linkages around Zr and ZrO_2 loading; high dispersion of ZrO_2 at low content is favorable for the factor controlling the former. Then the balance between the two factors leads to the maximum acidity in the range of 2–5% loading. The Lewis acidity correlates with the g_1 value of adsorbed O_2^- on ZrO_2/SiO_2 which will be described later.

Table 1
Acid strength of ZrO_2/SiO_2.

Zr (mol%)	Acid strength[a] (H_0)
1	+3.3 to +4.8
2	−8.2 to −5.6
5	−8.2 to −5.6
10	−8.2 to −5.6
20	−8.2 to −5.6
100	+4.8<

[a] Hammett acidity function.

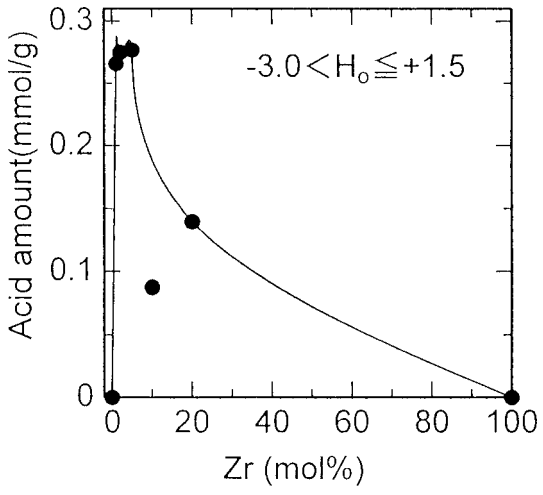

Figure 1. Plot of acid ($-3.0 < H_0 < +1.5$) amount *vs.* ZrO_2 loading.

3.2. XANES spectra

XANES spectra of four standard Zr compounds are shown in figure 2(a): $Zr(OBu^t)_4$ (tetrahedral), ZrO_2 (seven coordinated), $ZrSiO_4$ (eight coordinated, 4 × short Zr–O bonds, 4 × long Zr–O bonds), $Zr(acac)_4$ (acac = acetylacetonate, eight coordinated). The pre-edge peak is assigned to a 1s-to-4d transition with p–d mixing [11,12]. The pre-edge peak can discriminate tetrahedral Zr from higher coordinated Zr species though the peak height of a tetrahedral Zr compound is not as large as those of tetrahedral Ti compounds [13].

Figure 2(b) shows XANES spectra of 1–10 mol% ZrO_2/SiO_2 which were heated *in vacuo* at 493 K for 1 h prior to measurements. The pre-edge peak diminishes and the shape in the region of 18.00–18.04 keV changes with an increase in ZrO_2 content. The pre-edge peak area was estimated by the deconvolution of a spectrum in a similar way to that described earlier [14]. The area is the largest at 1 mol% ZrO_2 and decreases gradually with the increase in ZrO_2 content (figure 3). When we assume that the pre-edge peak is indicative of coordinatively unsaturated Zr species, ZrO_2/SiO_2 with less than 5 mol% ZrO_2 has an abundance of it. Without heat-treatment the pre-edge peak areas of 1–20 mol% ZrO_2/SiO_2 are lowered by a factor of 0.7–0.8; adsorption of water on coordinatively unsaturated ZrO_2/SiO_2 diminishes the pre-edge peak. Similar XANES changes were observed for zirconia–silica xerogels [11].

Fourier transform spectra are shown for 1–10 mol% ZrO_2/SiO_2 together with those of standard Zr compounds (figure 4). Since they were not corrected for phase-shift, the Zr–O and Zr–Zr distances should be longer than the peak positions in the figure. $Zr(OBu^t)_4$ has tetrahedral configuration with the shortest bond distance of 0.185 nm [15]. The Zr–O peak positions of seven and eight coordinated compounds are almost the same for ZrO_2 (0.203 nm × 3, 0.221 nm × 4), $ZrSiO_4$ (0.213 nm × 4, 0.227 nm × 4) and $Zr(acac)_4$ (0.220 nm × 8).

ZrO_2/SiO_2 was evacuated at 473 K for 2 h prior to XAFS measurement. The Zr–O peak distance of 1 mol% ZrO_2/SiO_2 is slightly shorter than those of higher loaded ZrO_2/SiO_2 and ZrO_2 itself, but longer than that of $Zr(OBu^t)_4$. The second peak positions of ZrO_2/SiO_2, which are different from that of authentic ZrO_2, should be assigned to Zr–O–Si [12]. Precise curve fitting could not be done because of the noisy spectra. The heights of the first and the second peaks slightly increase with the increase of Zr content, which suggests the increased coordination number. Coor-

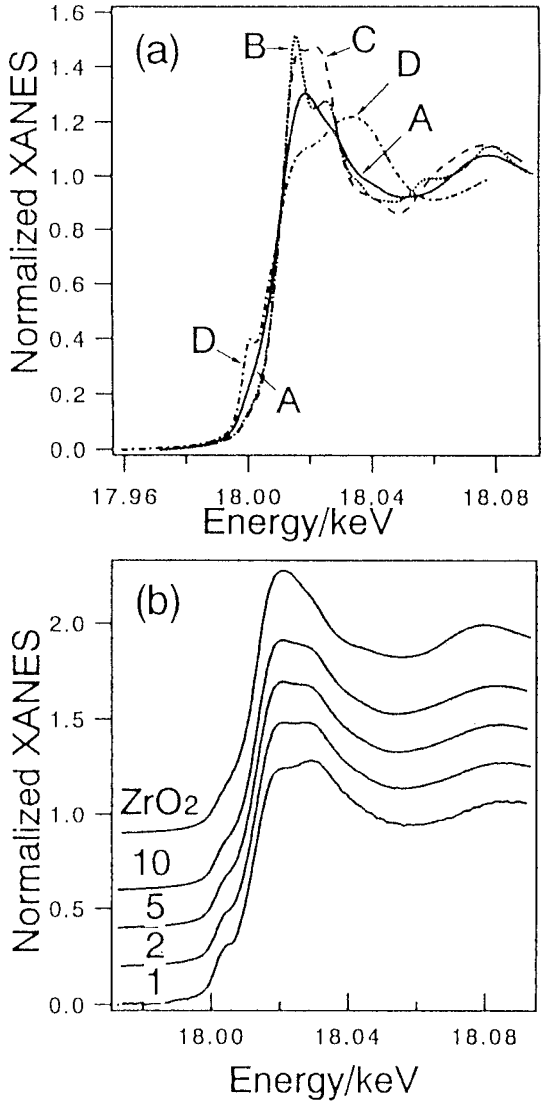

Figure 2. XANES spectra of Zr K edge. (a) Standard zirconium compounds: (A) ZrO_2, (B) $ZrSiO_4$, (C) $Zr(acac)_4$ and (D) $Zr(OBu^t)_4$; (b) ZrO_2/SiO_2. The figure shows the amount of loading (mol%).

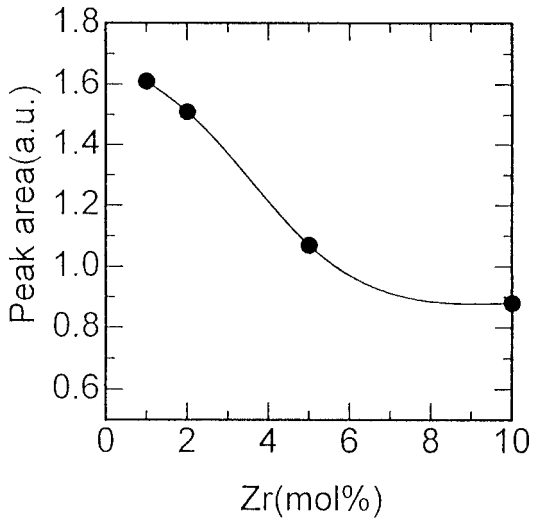

Figure 3. Plot of pre-edge peak area of Zr K edge *vs.* ZrO_2 loading.

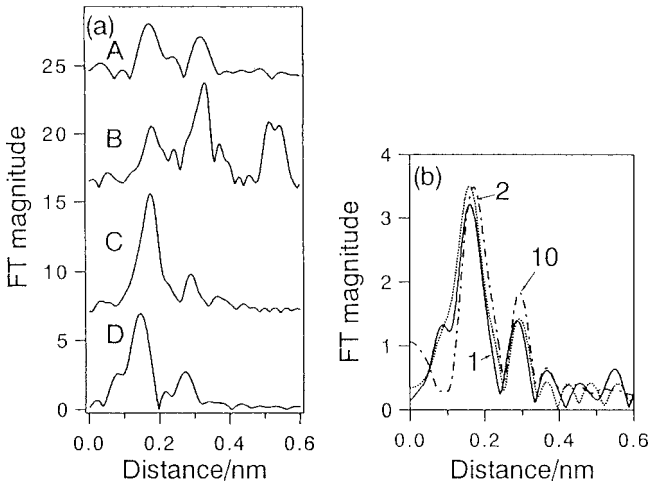

Figure 4. Fourier transforms. (a) Standard zirconium compounds: (A) ZrO_2, (B) $ZrSiO_4$, (C) $Zr(acac)_4$ and (D) $Zr(OBu^t)_4$; (b) ZrO_2/SiO_2. The figure is loading mol%.

dinatively unsaturated species of Zr is more abundant for 1 mol% ZrO_2/SiO_2 than for higher loaded ZrO_2/SiO_2.

3.3. ESR spectra

When TBHP in benzene solution was reacted with ZrO_2/SiO_2 in an ESR tube under N_2 for 3 h, followed by evacuation at 293 K, anisotropic signals assigned to O_2^- were formed. The g_1 values at the lowest magnetic field change with the amount of ZrO_2 loading (figure 5); the lower the loading, the lower the g_1 value. The situation is similar to that of the pre-edge peak area of the XANES spectrum. A possibility of O_2^- production from TBHP and ZrO_2 was assumed by Giamello *et al.* [16]. Although the O_2^- signal intensity still remained on exposure of propylene at 293 K, it decayed in the presence of 1-octene at 343 K with a half-life of 2.8 min.

3.4. Epoxidation of 1-octene with TBHP

Epoxidation of 1-octene was carried out with TBHP at 343 K over ZrO_2/SiO_2 for 3 h (table 2). The epoxidation selectivity is defined as the ratio of the amount of produced 1,2-epoxyoctane to that of the reacted TBHP. The rate of epoxidation is rather faster than that over TiO_2/SiO_2 prepared by a rapid hydrolysis method [4]. Furthermore, the selectivity of epoxide formation on ZrO_2/SiO_2 with less than 10 mol% loading is as high as that over low-loaded TiO_2/SiO_2. TBHP itself was slowly decomposed at 343 K in the absence of 1-octene by ZrO_2/SiO_2. Since Zr in low-loaded ZrO_2/SiO_2 takes a coordinatively unsaturated configuration as described earlier, coordinatively unsaturated Zr species is responsible for the selective epoxidation. The epoxidation rate defined as the rate of production of 1,2-epoxyoctane per 1 g of catalyst is plotted against Zr content together with pre-edge peak area and g_1 value on the ordinate (figure 6). The parallelism among the epoxidation rate, the pre-edge peak area of Zr K-edge XANES and the g_1

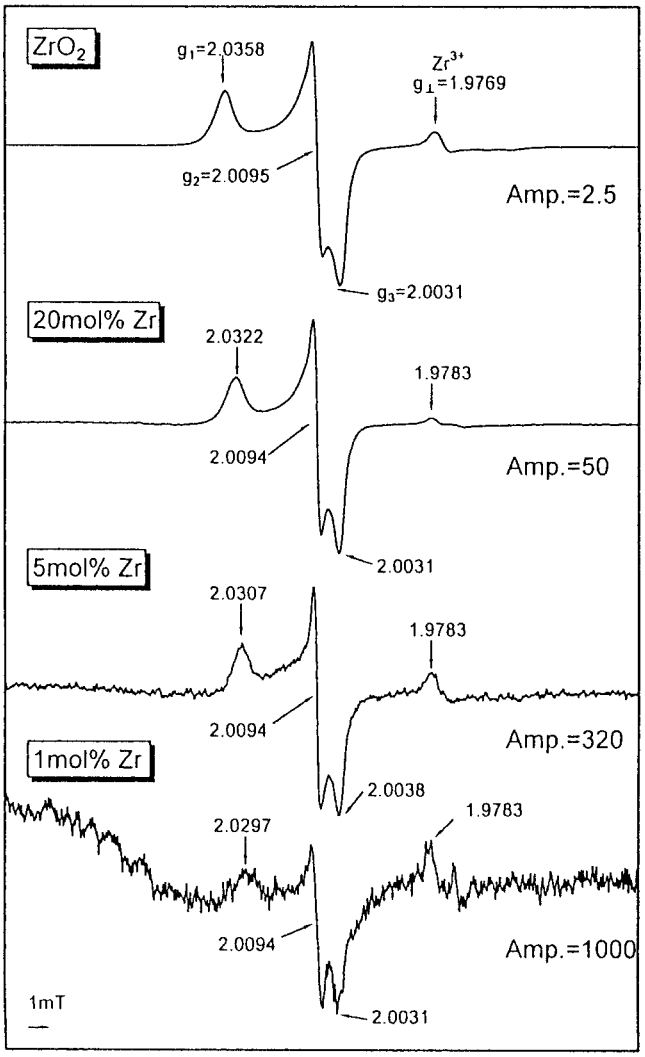

Figure 5. ESR spectra of O_2^- generated from the reaction of TBHP with ZrO_2/SiO_2.

Table 2
Oxidation of 1-octene with TBHP catalyzed by ZrO_2/SiO_2 (343 K, 3 h).

Zr (mol%)	TBHP conversion (%)	Epoxide selectivity (%)
1	82.4	100
2	77.3	100
5	79.9	100
10	71.3	100
20	46.0	40.1
100	50.8	0

value of the O_2^- ESR spectrum supports the conclusion that the active species for epoxidation of 1-octene with TBHP is coordainatively unsaturated ZrO_2 dipersed on Aerosil-SiO_2.

We carried out epoxidation of 1-octene with TBHP over ZrO_2/SiO_2 prepared by a sol–gel method from $Zr(OBu^n)_4$ and $Si(OC_2H_5)_4$ [7]. The highest epoxide selectivity was 59% over 0.5 mol% ZrO_2/SiO_2. Few catalysts surpassed the selectivity attained by ZrO_2/Aerosil-SiO_2. Compared with the role of SiO_2 (abbreviated as hydro-SiO_2) prepared

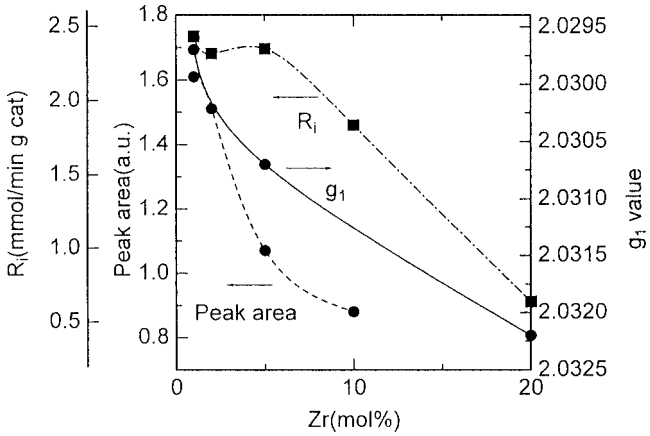

Figure 6. Relationship between epoxidation rate, pre-edge peak area of XANES of Zr K edge and ESR g_1 value of O_2^- signal.

by hydrolysis of $Si(OC_2H_5)_4$, the crucial effect of Aerosil-SiO_2 has not been decisively determined. Low-loaded ZrO_2 on hydro-SiO_2 revealed that pre-edge peak areas assigned to the coordinatively unsaturated configuration remained almost constant irrespective of loading up to 50 mol% [7]. Aerosil-SiO_2 which was manufactured by thermolysis from $SiCl_4$ in a H_2–O_2 mixture at Nippon Aerosil Co. is an ultrafine and hydrophilic powder [17]. Its surface area is as large as that of commercial SiO_2 and rather smaller than that of hydro-SiO_2. As speculated earlier, coordinatively unsaturated Zr species are responsible for epoxidation of olefins with TBHP. Although we cannot estimate the ratio of tetrahedral to octahedral species for ZrO_2/SiO_2 from XAFS and ESR data, the former should be more active for the reaction of TBHP since the conversion of TBHP over 1 mol% ZrO_2/SiO_2 is higher than that over higher loaded ZrO_2/SiO_2.

This work reveals that supports prepared by different methods provide different behavior in selective oxidation. We are exploring why ZrO_2/Aerosil-SiO_2 is more selective in epoxidation of 1-octene with TBHP than ZrO_2–SiO_2 composite oxides prepared by a rapid sol–gel method [7].

Acknowledgement

This work was supported by the Ministry of International Trade and Industry (MITI) and the New Energy and Industrial Technology Development Organization (NEDO) of Japan. The XAFS measurements were performed under the approval of the Photon Factory Program Advisory Committee (Proposal No. 96P009). We are grateful to Professor Nomura of IMSS (KEK) for XAFS measurements. We thank Mr. Matsuyama of Nippon Oil and Fats Co. for valuable discussions and for providing *tert*-butyl hydroperoxide.

References

[1] R.A. Sheldon, in: *Catalytic Oxidation – Principles and Applications*, eds. R.A. Sheldon and R.A. van Santen (World Scientific, Singapore, 1995) p. 175.

[2] T. Hayashi, K. Tanaka and M. Haruta, J. Catal. 178 (1998) 566.
[3] S. Imamura, T. Nakai, H. Kanai and T. Ito, Catal. Lett. 28 (1994) 277.
[4] S. Imamura, T. Nakai, H. Kanai and T. Ito, J. Chem. Soc. Faraday Trans. 91 (1995) 1261.
[5] H. Kanai, M. Shono, S. Imamura and H. Kobayashi, J. Mol. Catal. A 130 (1998) 187.
[6] S. Imamura, H. Sasaki, M. Shono and H. Kanai, J. Catal. 177 (1998) 72.
[7] S. Imamura, T. Yamashita, K. Hamada and H. Kanai, React. Kinet. Catal. Lett. 72 (2001) 11.
[8] F. Wattimena and Wulff, Ger. Offen. 2 015 505 (1971); Chem. Abstr. 73 (1970) 120,185.
[9] Japan Society of Analytical Chemistry, ed., *Bunsekikagaku Benran* (Maruzen, 1981) p. 334.
[10] Z. Dang, B.G. Anderson, Y. Amenomiya and B.A. Morrow, J. Phys. Chem. 99 (1995) 14437.
[11] G. Mountjoy, D.M. Pickup, R. Anderson, G.W. Wallidge, M.A. Holland, R.J. Newport and M.E. Smith, Phys. Chem. Chem. Phys. 2 (2000) 2455.
[12] K. Okumura and Y. Iwasawa, J. Catal. 164 (1996) 440.
[13] H. Kanai and H. Kobayashi, Catal. Lett. 20 (1993) 125.
[14] S. Yoshida, T. Tanaka, T. Hanada, T. Hiraiwa, H. Kanai and T. Funabiki, Catal. Lett. 12 (1992) 277.
[15] S.L. Latesky, J. Keddington, A.K. Mcmullen, I.P. Rothwell and J.C. Huffman, Inorg. Chem. 24 (1985) 995.
[16] E. Giamello, M. Volante, B. Fubini, F. Geobaldo and C. Morterra, Mater. Chem. Phys. 29 (1991) 379.
[17] T. Takei, M. Ataku, T. Konishi, M. Fuji, T. Watanabe and M. Chikazawa, Funtai Kagaku Kaishi 36 (1999) 179.